

1 Title: LDER-GE estimates phenotypic variance component of gene-environment interactions in  
2 human complex traits accurately with GE interaction summary statistics and full LD information  
3

4 Authors: Zihan Dong, MS<sup>1,2,\*</sup>, Wei Jiang, PhD<sup>1,\*</sup>, Hongyu Li, PhD<sup>1</sup>, Andrew T. DeWan, PhD<sup>2,3,†</sup>,  
5 Hongyu Zhao, PhD<sup>1,†</sup>

6 <sup>1</sup>Department of Biostatistics, Yale School of Public Health, New Haven, CT

7 <sup>2</sup>Center for Perinatal, Pediatric and Environmental Epidemiology, Yale School of Public Health,  
8 New Haven, CT

9 <sup>3</sup>Department of Chronic Disease Epidemiology, Yale School of Public Health, New Haven, CT

10

11 \* These authors contributed equally to this work.

12 † These authors share senior authorship.

13

14 Corresponding Authors: Hongyu Zhao, Department of Biostatistics, Yale School of Public Health,  
15 300 George Street, 5th floor, New Haven, CT 06511, Telephone: 203-785-3613, Fax: 203-785-  
16 6912, Email: hongyu.zhao@yale.edu

17 Andrew T. DeWan, Yale Center for Perinatal, Pediatric and Environmental Epidemiology, Yale  
18 School of Public Health, 1 Church Street, 6th Floor, New Haven, CT 06520, Telephone: 203-  
19 785-3528, Fax: 203-785-6279, Email: andrew.dewan@yale.edu

20

21 Conflict of Interest: None

22

23 Keywords: Gene-environment interaction, genome-wide interaction scan, missing heritability,  
24 linkage disequilibrium, statistical efficiency

25 Abbreviations: GE: gene-environment. GWIS: genome-wide interaction scan. LD: linkage  
26 disequilibrium. SNP: single nucleotide polymorphism. E-Y pair: environmental covariate  
27 phenotype pair.

28 Word count: 3894 (excluding abstract)

29 Figures: 3

30 Tables: 4

31 Code and data availability: “LDER-GE” and pre-computed LD information can be found at  
32 <https://github.com/shuangs0110/LDER>.

33

34

35 **Abstract**

36 Gene-environment (GE) interactions are essential in understanding human complex traits.  
37 Identifying these interactions is necessary for deciphering the biological basis of such traits. In  
38 this study, we introduce a statistical method Linkage-Disequilibrium Eigenvalue Regression for  
39 Gene-Environment interactions (LDER-GE). LDER-GE improves the accuracy of estimating the  
40 phenotypic variance component explained by genome-wide GE interactions using large-scale  
41 biobank association summary statistics. LDER-GE leverages the complete Linkage  
42 Disequilibrium (LD) matrix, as opposed to only the diagonal squared LD matrix utilized by LDSC  
43 (Linkage Disequilibrium Score)-based methods. Our extensive simulation studies demonstrate  
44 that LDER-GE performs better than LDSC-based approaches by enhancing statistical efficiency  
45 by approximately 23%. This improvement is equivalent to a sample size increase of around 51%.  
46 Additionally, LDER-GE effectively controls type-I error rate and produces unbiased results. We  
47 conducted an analysis using UK Biobank data, comprising 307,259 unrelated European-  
48 Ancestry subjects and 966,766 variants, across 151 environmental covariate-phenotype (E-Y)  
49 pairs. LDER-GE identified 35 significant E-Y pairs while LDSC-based method only identified 25  
50 significant E-Y pairs with 23 overlapped with LDER-GE. Furthermore, we employed LDER-GE  
51 to estimate the aggregated variance component attributed to multiple GE interactions, leading to  
52 an increase in the explained phenotypic variance with GE interactions compared to considering  
53 main genetic effects only. Our results suggest the importance of impacts of GE interactions on  
54 human complex traits.

55

56 **Introduction**

57 A growing body of literature underscores the significant role of gene-environment (GE)  
58 interactions in shaping human complex traits<sup>1-4</sup>. The exploration of GE interactions may  
59 elucidate a portion of the 'missing heritability'<sup>5</sup> — the phenotypic variance not accounted for by  
60 known genetic effects. Additionally, the inference of GE interactions and their effects can  
61 contribute to our understanding of human disease etiology and mechanisms<sup>6</sup>, and enhance our  
62 ability to assess risk and identify high-risk individuals, ultimately supporting the development of  
63 personalized medicine<sup>1</sup>. Traditionally, environmental exposure variables have been limited to  
64 factors like environmental toxins, air pollutants, or viral infections<sup>6</sup>. However, some gene-  
65 environment interaction studies<sup>7,8</sup> also consider other variables, heritable or non-heritable, such  
66 as sex, as environmental exposure variables. In this study, we adopt a broad definition,  
67 considering both non-heritable covariates and heritable phenotypes as environment interactive  
68 variables, as previously discussed<sup>2</sup>.

69

70 Numerous methods and tools have been developed to investigate GE interactions from various  
71 angles. One such approach is the genome-wide interaction scan (GWIS), which estimates the  
72 interaction effect<sup>9</sup> between individual genetic variants and environmental factors through  
73 regression. GWIS generates interaction summary statistics for each variant, akin to  
74 conventional genome-wide association studies (GWAS). However, we note that GE interaction  
75 effect sizes tend to be smaller than genetic main effects<sup>10</sup>. Consequently, this can lead to  
76 reduced statistical power, particularly when challenged by the multiple testing burden across the  
77 entire genome<sup>11</sup>. Several studies have directed their efforts towards estimating the genome-  
78 wide contribution of GE interactions through diverse statistical approaches. One such method is  
79 the Gene-Environment Interaction Genomic Restricted Maximum Likelihood (GEI-GREML),  
80 which leverages restricted maximum likelihood estimation by pre-computing the correlation  
81 matrix of the GE term across samples<sup>12</sup>. On the other hand, the Multivariate Reaction Norm  
82 Model (MRNM) is a reaction norm model that has the capability to distinguish between GE  
83 interaction and GE correlation<sup>13</sup>. Both GEI-GREML and MRNM necessitate individual-level  
84 genotype data and can be computationally demanding and time-consuming, especially when  
85 dealing with extensive biobank datasets.

86

87 To tackle these challenges, researchers have devised alternative methods that make use of  
88 GWIS summary statistics. Notably, methods like PIGEON<sup>7</sup> and GxEsum<sup>8</sup> build upon the  
89 principles of LD-score regression (LDSC)<sup>14</sup>. They harness partial linkage disequilibrium (LD)  
90 information among genetic variants to estimate the phenotypic impact of GE interactions using  
91 the method of moments. However, this approach often results in reduced statistical efficiency  
92 when estimating variance components, because the phenotypic variance attributed to GE  
93 interactions is often considerably smaller than the narrow-sense heritability. For example,  
94 across a dataset encompassing more than 500 traits, the phenotypic variance explained by  
95 genetic-sex interactions typically falls within the range of 0% to a maximum of 2%<sup>7</sup>. While this  
96 may appear modest, acknowledging and investigating this component remains important for our  
97 understanding of complex traits and disease etiology. An inefficient estimation method may fail  
98 to detect the contribution of GE interactions. Consequently, there is a need for a more efficient  
99 approach to estimate the phenotypic variance explained by GE interactions while effectively  
100 managing computational demands. Current LDSC-based frameworks<sup>7,8,14</sup> make use of the  
101 squared variant LD matrix but primarily focus on diagonal information. Previous research<sup>15,16</sup>  
102 has convincingly shown that incorporating the complete LD information can substantially

103 enhance the efficiency of estimating narrow-sense heritability under the genetic additive effect  
104 model. Building upon this insight, we introduce the Linkage-Disequilibrium Eigenvalue  
105 Regression for Gene-environment interactions (LDER-GE) to estimate the genome-level GE  
106 interaction variance component more efficiently.

107

108 LDER-GE mimics the original LDER framework<sup>15</sup>, which harnesses the full potential of LD  
109 information through eigen-decomposition of the LD matrix. This process transforms the original  
110 GWIS summary statistics and consolidates the association information. Notably, LDER-GE  
111 relies on summary statistics and the LD matrix constructed using a reference panel.  
112 Consequently, it efficiently manages large-scale Biobank data without imposing substantial  
113 computational demand. Extensive simulations provide evidence that both LDER-GE and the  
114 LDSC-based method effectively control the type-I error rate and deliver unbiased estimates.  
115 However, LDER-GE excels in terms of statistical efficiency compared to the LDSC-based  
116 method in all simulation scenarios. In a real-data application involving 151 E-Y pairs from the  
117 UK-Biobank<sup>17</sup>, the LDSC-based method identified 25 GE interaction signals, whereas LDER-GE  
118 identified 35 E-Y pairs (40% increase). For a more precise assessment of the contribution of GE  
119 interactions to missing heritability, we estimate the aggregated GE interaction variance involving  
120 multiple environmental covariates and the analyzed phenotypes. In this regard, LDER-GE  
121 facilitates more accurate estimation. In summary, the missing heritability contributed by the  
122 aggregated multi-covariate GE interaction variance represents a substantial addition to the  
123 narrow-sense heritability.

124

## 125 **Results**

### 126 **Method overview**

127 We propose LDER-GE to improve statistical efficiency with summary-level association statistics.  
128 Under the polygenic GE model where each standardized variant-by-E term has small effect, the  
129 expectation of cross-variant level GE interaction association chi-square statistics is (details in  
130 methods and supplementary note 1)

$$E(\mathbf{Z}\mathbf{Z}^T) = Nh_I^2 \mathbf{L}/M + (c + 2(h_I^2 + \sigma_1^2)) \mathbf{R}, \quad (1)$$

131 where  $\mathbf{Z}$  is the original GWIS Z-score vector,  $\mathbf{R}$  is the LD matrix,  $\mathbf{L} = \mathbf{R}^T \mathbf{R}$  is the LD score matrix,  
132  $N$  is the sample size of the GWAS summary statistics,  $c$  is the unconstrained intercept with  
133 potential inflation,  $\sigma_1^2$  is the non-genetic environment interaction variance and  $h_I^2$  is the explained  
134 variance of the GE interaction. We incorporate full LD information by conducting eigen-  
135 decompose the LD matrix as  $\mathbf{R} = \mathbf{U}\mathbf{D}\mathbf{U}^T$ , with  $\mathbf{U}$  being the orthogonal matrix of eigenvectors and

136 **D** being the diagonal eigen value matrix, and transforming the original GWIS Z-score vector **Z**:  $\tilde{\mathbf{Z}}$   
137  $= \mathbf{D}^{-1/2} \mathbf{U}^T \mathbf{Z}$ , yielding

$$E(\tilde{Z}_j^2) = Nh_I^2 D_{jj}/M + (c + 2(h_I^2 + \sigma_1^2)). \quad (2)$$

138 We run iterative weighted least squares to estimate  $h_I^2$  and the intercept, followed by delete-  
139 block-wise jackknife to estimate the standard error.

140

#### 141 **Simulation results using real genotype panel**

142 Figure 1 and Table 1 compare the performance of LDER-GE and the LDSC-based method  
143 across various parameter combinations. Across all simulation scenarios, the LDER-GE method  
144 consistently had better performance than the LDSC-based method, whether utilizing an UKBB  
145 in-sample or 1000 Genomes project out-sample reference panel. We assessed performance  
146 using precision, which is the inverse of the standard deviation, and root mean squared error.  
147 Notably, this precision improvement was, on average, equivalent to a 51% increase in sample  
148 size when analyzing continuous simulated phenotypes during in-sample estimation. Table 2  
149 shows that the type-I error rates were well-controlled for all three methods: LDER-GE using an  
150 in-sample LD panel, LDER-GE using an out-sample LD panel, and LDSC-based in-sample LD  
151 panel. This held true both in scenarios with and without the presence of non-genetic residual-  
152 environment interaction effects.

153

154 The transformation from observed-scale variance to liability-scale variance, as achieved by the  
155 Roberston transformation<sup>18</sup>, relies on the normality assumption of the liability distribution.  
156 However, this assumption is violated with the non-normal GE term. Our simulations, considering  
157 various prevalence and GE interaction variance settings, suggest that the transformation  
158 provides reasonably unbiased results (S. Figure 1, Panels B, C, and D) when the disease is not  
159 rare, with a prevalence exceeding 10%, or when the GE interaction variance remains relatively  
160 small, at or below 5%. Nevertheless, in cases where the disease is rare, and the GE interaction  
161 variance is non-trivial (S. Figure 1, Panels A and B), the transformed liability-scale GE  
162 interaction variance estimate tends to be overestimated. This trend becomes more pronounced  
163 as the disease prevalence decreases. Despite the potential bias introduced by the Roberston  
164 transformation<sup>18</sup> in the presence of the GE term, the type-I error rate for tests involving binary  
165 phenotypes remained well-controlled (Table 3) across varying prevalence settings. Our findings  
166 related to the estimation of GE liability-scale variance and the results of type-I error rate  
167 simulations for binary phenotypes align with a previous study<sup>8</sup>, except that LDER-GE achieved

168 better estimation accuracy than LDSC-based method using in-sample and out-sample LD  
169 reference panels (S Table 1).

170

## 171 **Real data analysis using UKBB data**

172 We examined 151 E-Y pairs involving 307,259 unrelated European ancestry individuals and a  
173 total of 966,766 genetic variants from the UK Biobank (UKBB). We employed both the LDER-  
174 GE and LDSC-based methods. Following Bonferroni correction, LDER-GE identified 35  
175 significant pairs, of which 23 overlapped with the 25 pairs identified by the LDSC-based method  
176 (Figure 2). Further details about the 12 E-Y pairs exclusively identified by LDER-GE and the two  
177 E-Y pairs uniquely identified by the LDSC-based method can be found in S Table 2. Previous  
178 research has provided evidence of gene-age interaction effects on blood pressure through  
179 extensive GWAS data from three blood pressure consortia<sup>19</sup> and linkage analysis<sup>20</sup>. In our  
180 analysis, LDER-GE successfully captured signals from both systolic blood pressure (SBP) and  
181 diastolic blood pressure (DBP), while the LDSC-based method failed to detect the DBP signal.  
182 Additionally, gene-sex interaction effects have been reported for traits such as height<sup>21</sup>,  
183 depression<sup>22,23</sup> and cholesterol level<sup>24</sup>, all of which were exclusively detected by LDER-GE. In  
184 summary, the estimated values obtained using LDER-GE and the LDSC-based method  
185 exhibited strong overall consistency. However, we note that the standard error of LDER-GE was,  
186 on average, 21% lower than that of the LDSC-based method, a result consistent with our  
187 simulation findings. For a comprehensive overview of the analysis results for all 151 E-Y pairs,  
188 see S Table 3. Among the seven environmental covariates investigated, sex, Body Mass Index  
189 (BMI), and age exhibited relatively larger genome-level GE interaction effects and lower P-  
190 values compared to the other covariates (S Table 3). On the other hand, the pollution covariate  
191 pm2.5 did not exhibit statistically significant GE interactions across all tested phenotypes,  
192 including several lung-related traits. This can be a consequence of small GE interaction  
193 magnitudes and inaccuracy of air pollution indicator measurements.

194

195 For each of the 22 phenotypes, we estimated the aggregated multi-GE interaction variance  
196 using ordered covariates (age, sex, BMI, packed years of smoking, Townsend deprivation index,  
197 alcohol intake frequency). Post Bonferroni correction, LDSC-based method identified 13  
198 phenotypes, while LDER-GE identified 16 phenotypes which covered all the 13 phenotypes  
199 discovered by LDSC-based method (S Table 4, S Figure 2). The additional 3 phenotypes  
200 identified are height, normalized FVC and neuroticism score, whose aggregated GE interaction  
201 variances were estimated around 1%. Notably, some phenotypes like depression and male

202 genital tract cancer exhibited significant single-covariate GE interactions but were not detected  
203 with multi-GE interaction variance. This discrepancy may be due to noise introduced by other  
204 weak covariates during multi-covariate aggregation. Similar to single-covariate GE analysis,  
205 LDER-GE consistently yielded results comparable to the LDSC-based method in assessing  
206 multi-GE interaction variance but reported an average standard error 21% smaller than the  
207 LDSC-based method. We also estimated narrow-sense heritability  $h^2$  and compared it to the  
208 aggregated multi-GE interaction variance. Notably, 13 of the 22 phenotypes exhibited  
209 substantial multi-GE interaction variance, contributing more than 10% relatively to the narrow-  
210 sense heritability. For conditions like type-II diabetes (T2D) and coronary artery disease (CAD),  
211 the multi-GE interaction variance approached the magnitude of the narrow-sense heritability,  
212 providing valuable insights into disease etiology. However, we caution that when interpreting  
213 results for binary diseases, as the liability-scale transformation may introduce bias. We reversed  
214 the covariate order and used the set (alcohol intake frequency, Townsend deprivation index,  
215 packed years of smoking, BMI, sex, age) for the same analysis. It turned out that the order of  
216 covariates did not substantially affect the results (S Table 5).

217

## 218 **Discussion**

219 In this study, we introduce LDER-GE to improve the precision of estimating GE interaction  
220 variance of complex traits using summary statistics. LDER-GE leverages full LD information  
221 from the LD panel while LDSC-based methods<sup>7,8</sup> rely solely on the LD panel's diagonal  
222 information. Our simulations and analysis of UK Biobank data demonstrate LDER-GE's  
223 superiority over LDSC-based approaches in terms of estimation accuracy and root mean square  
224 error. LDER-GE's improved accuracy enables the detection of more genome-level GE  
225 interactions that might go undetected by LDSC-based methods.

226

227 From real data analysis, sex and BMI had more detectable GE interaction effects over various  
228 health-related traits, consistent with results from other studies. For example, several studies  
229 reported that sex modifies genetic effects on lipid traits<sup>25</sup>, obesity<sup>26,27</sup>, and hypertension<sup>28</sup> from  
230 different perspectives. BMI is known to be causal to multiple health-related traits such as T2D  
231 and hypertension<sup>29,30</sup>, part of which could be reasoned from the GE interaction effects<sup>8</sup>. While  
232 biological sex is almost fixed for most individuals in the population throughout the lifetime as  
233 well as its associated GE interaction variance, BMI varies during different life stages. The gene-  
234 BMI interaction study potentially brings additional significance to the clinical prevention or  
235 treatment to diseases such as T2D and hypertension, given their considerable GE interaction

236 variance estimate. The higher statistical efficiency of LDER-GE allows us to better estimate the  
237 aggregated multi-GE interaction variance, which is comparable to narrow sense heritability,  
238 especially for T2D and Coronary Artery Disease (CAD). However, such interpretation must be  
239 accompanied with caution, due to the normality and additive effect assumption violations of  
240 Roberston transformation<sup>18,31,32</sup>. Empirically, simulations demonstrate the true aggregated multi-  
241 GE interaction variance is lower than the transformed liability-scale variance when the disease  
242 is rare (<=5%), but the magnitude difference is not considerable.

243

244 Our real data analysis highlighted the significant gene by SEX and gene by BMI interaction  
245 effects over various health-related traits, a finding consistent with diverse studies. For instance,  
246 sex has been shown to modify genetic effects on traits like lipid<sup>25</sup>, obesity<sup>26,27</sup>, and  
247 hypertension<sup>28</sup>. Additionally, BMI, a known causal factor for multiple health-related traits such as  
248 T2D and hypertension<sup>29,30</sup>, may exert some of its influence through gene-environment (GE)  
249 interactions<sup>8</sup>. While biological sex remains relatively constant throughout an individual's lifetime,  
250 BMI is subject to regulation. Investigating BMI's GE interaction implications could have clinical  
251 significance, particularly in preventing or treating diseases like T2D and hypertension, given  
252 their substantial GE interaction variance estimates. LDER-GE's enhanced statistical efficiency  
253 enables more accurate estimation of aggregated multi-GE interaction variance, which, notably,  
254 often approaches the magnitude of narrow-sense heritability, especially for T2D and CAD.  
255 However, it's crucial to exercise caution in interpreting these findings, as they hinge on the  
256 normality and additive effect assumptions of the Roberston transformation<sup>18,31,32</sup>. Empirical  
257 simulations reveal that in cases of rare diseases (prevalence <= 5%), the true aggregated multi-  
258 GE interaction variance tends to be lower than the estimated liability-scale variance, though the  
259 difference in magnitude is not substantial.

260

261 As previously discussed<sup>8</sup>, it's not recommended to directly estimate the non-genetic-residual-  
262 environment interaction variance from the intercept using the formula (intercept – 2\*h<sub>i</sub><sup>2</sup>)/2. This  
263 is because the intercept can be inflated by factors such as population stratification and other  
264 confounding effects, making it difficult to separate from the non-genetic-residual-environment  
265 interaction variance. When analyzing binary phenotypes, there's the additional challenge of  
266 unknown prevalence differences between the sampling population and the target population,  
267 which can further inflate the estimated intercept<sup>14</sup>.

268

269 To expedite computation, we partitioned the entire genome into 1009 approximately  
270 independent blocks based on their LD relationships. We derived the block-wise LD matrix using  
271 a dataset of 307,259 individuals of European ancestry from the UK Biobank. Alternatively, we  
272 also calculated the out-sample LD matrix using 489 subjects from the 1000 Genomes project<sup>33</sup>,  
273 employing a linear shrinkage method<sup>34,35</sup>, and the 1703 genomic blocks from LDetect<sup>36</sup>.  
274 Typically, the 1000 Genomes project reference panel is utilized when in-sample LD information  
275 is unavailable. For readers' convenience, both computed panels are accessible online. Our  
276 simulation results underscore the robustness of LDER-GE, whether LD panels are constructed  
277 from the UK Biobank or the 1000 Genomes project. However, it's advisable to prioritize the UK  
278 Biobank reference when there's a significant overlap between the variants in the GWIS input  
279 summary statistics and the UK Biobank reference panel, mainly due to its larger sample size.  
280

281 As an extension of the LDSC-based method, LDER-GE inherits most of its limitations. Firstly, it  
282 assumes polygenic GE effects on the phenotype, and a violation of this assumption can result in  
283 underestimation of the variance component<sup>37</sup>. Secondly, our model does not differentiate  
284 between GE covariate correlations, potentially introducing estimation bias due to  
285 overadjustment<sup>8</sup>. Methods addressing such correlations are available<sup>13</sup>. Thirdly, LDER-GE has  
286 not been applied to case-control studies, which often involve oversampling of cases. While  
287 efforts are being made to address these limitations, future research could explore incorporating  
288 variant functional annotation or allele frequency information to enhance estimation<sup>37</sup>.  
289

290 To summarize, LDER-GE utilizes full LD information and summary statistics to estimate the  
291 phenotypic variance explained by GE interactions more accurately than LDSC-based estimation  
292 methods. LDER-GE controls the computational burden and time well compared to methods that  
293 requires individual-level data input and can be employed to estimate multiple E-Y pairs of large  
294 sample size.  
295

## 296 **Material & methods**

### 297 **LDER-GE modelling & estimation**

298 We consider the following model

$$Y_i = \sum_{j=1}^M G_{ji} \beta_j + \sum_{j=1}^M S_{ji} \gamma_j + \epsilon_{1i} E_i + \epsilon_{0i}, \quad (3)$$

299 where  $Y_i$  is the phenotype for subject  $i$  already adjusted for fixed effects including the exposure  
300 covariate effects.  $E_i$  is the exposure covariate for subject  $i$ . Suppose there are  $M$  variants.  $G_{ji}$  is  
301 the  $j$ th variant for subject  $i$ .  $S_{ji} = G_{ji} * E_i$  is the GE interaction product term for variant  $j$  of subject  $i$ ,  
302  $\square_{1i}$  is the non-genetic residual that has exposure interaction effect.  $\square_{0i}$  is the residual  
303 independent from all other parts,  $\beta_j$  is the true additive genetic effect for variant  $j$ ,  $\gamma_j$  is the true  
304 interaction effect for variant  $j$ . Following PEGION's<sup>7</sup> setting, we model  $\beta_j$  and  $\gamma_j$  using the  
305 following random effects model:

$$\beta_j \sim N(0, h_g^2/M),$$

$$\gamma_j \sim N(0, h_I^2/M),$$

306 where  $h_g^2$  is the narrow-sense heritability and  $h_I^2$  is the GE interaction variance that we are  
307 interested in estimating. And  $\beta_j$  and  $\gamma_j$  may or not be correlated. We model  $\square_0$  and  $\square_1$  using  
308 random effects model:

$$\epsilon_0 \sim N(0, \sigma_0^2),$$

$$\epsilon_1 \sim N(0, \sigma_1^2),$$

310 where  $\sigma_1^2$  is the non-genetic environment interaction variance. Again,  $\square_0$  and  $\square_1$  may or may not  
311 be correlated.

312 Under the polygenic GE model, we derive (supplementary note 1), in matrix form, that

$$E(\mathbf{Z}\mathbf{Z}^T) = Nh_I^2 \mathbf{L}/M + (c + (\mathbf{K}(E) - 1)(h_I^2 + \sigma_1^2)) \mathbf{R}, \quad (4)$$

$$E(\mathbf{Z}\mathbf{Z}^T) = Nh_I^2 \mathbf{L}/M + (c + 2(h_I^2 + \sigma_1^2)) \mathbf{R}, \quad (5)$$

313 where  $\mathbf{Z}$  is the GWIS Z-score vector,  $\mathbf{R}$  is the LD matrix,  $\mathbf{L} = \mathbf{R}^T \mathbf{R}$  is the LD score matrix,  $N$  is the  
314 sample size of the GWAS summary statistics,  $c$  is the unconstrained intercept with potential  
315 inflation and  $\mathbf{K}(E)$  is the kurtosis of the exposure covariate. In the case of  $E$  being standard  
316 normal, equation (4) reduces to the equation (5). Following the original LDER<sup>15</sup> framework, we  
317 eigen-decompose the LD matrix as  $\mathbf{R} = \mathbf{U}\mathbf{D}\mathbf{U}^T$ , where  $\mathbf{U}$  is the orthogonal matrix of eigenvectors  
318 and  $\mathbf{D}$  is the diagonal eigen value matrix. Then we transform the original GWIS Z-score vector  $\mathbf{Z}$ :  
319  $\tilde{\mathbf{Z}} = \mathbf{D}^{-1/2} \mathbf{U}^T \mathbf{Z}$  and have

$$E(\tilde{Z}_j^2) = Nh_I^2 D_{jj}/M + (c + 2(h_I^2 + \sigma_1^2)). \quad (6)$$

320 The transformed summary statistic vector contains all LD information, and the estimation  
321 efficiency is improved compared to LDSC-based methods as a consequence. The estimation  
322 task is accomplished using the iterative least squares and standard error is estimated using  
323 delete-block-wise jackknife.

324

328 To analyze binary outcomes, we transformed the observed-scale heritability to liability-scale  
329 heritability using Roberston transformation<sup>18</sup>. It has been pointed out that when the GE  
330 interaction variance is large, the normality assumption of the phenotype liability may be violated,  
331 resulting in biased results of Roberston transformation<sup>8,38</sup>. However, our simulation results  
332 showed that when the GE interaction variance proportion was small Roberston transformation  
333 still yielded reasonably accurate result (S Figure 1, S Table 1), consistent with previous studies<sup>8</sup>.  
334

335 The regression weight of the transformed summary statistics vector takes the same form as  
336 LDER<sup>15</sup> except the additional intercept inflation component (Supplementary note),

$$w_i = \min(D_{ii}, 1)/(1 + 2(h_I^2 + \sigma_1^2) + Nh_I^2 D_{ii}/M)^2, \quad (7)$$

337 where  $(1 + 2(h_I^2 + \sigma_1^2) + Nh_I^2 D_{ii}/M)^2$  is proportional to the variance of  $\bar{Z}_i$  (supplementary note 2)  
338 and the shrinkage operation  $\min(D_{ii}, 1)$  reduces the noise from big eigenvalues from LD matrix  
339 with lower sample sizes.

340

#### 341 **UKBB data for simulation and real data analysis**

342 The research conducted in this study utilized data from the UK Biobank Resource. The genomic  
343 partitioning and simulation analysis was conducted using UKBB dataset with application number  
344 29900. The real data analysis was conducted using UKBB dataset with application number  
345 32285. Detailed information regarding data access, ethical approval, quality control procedures,  
346 and phenotype definitions can be found in the supplementary note 2.

347

#### 348 **Reference panel construction:**

349 We first took the intersection between UKBB<sup>17</sup> imputed genotype panel, 1000 Genomes  
350 project<sup>33</sup> genotype panel and hapmap3 project<sup>39</sup> variant list, resulting in  $M = 396,330$  common  
351 variants. Then, we partitioned the entire human genome into 1009 roughly independent blocks  
352 using the panel of 396,330 common variants from UKBB European ancestry ( $N=276,050$ ). We  
353 partitioned the genome such that the linked SNP pairs (squared LD coefficient  $r^2 > 2/\sqrt{276050}$ )  
354 = 0.0038) are within 100 kilobases within each block. For simulations, in-sample reference  
355 panel was constructed using the intersected UKBB genotype panel ( $N=276,050$ ,  $M = 396,330$ )  
356 and the 1009 genomic blocks. Out-sample reference panel was constructed using the same set  
357 of variants but from 1000 Genome project genotype panel ( $N=489$ ,  $M = 396,330$ ), with the  
358 genome partition being the 1703 genomic blocks generated previously<sup>15</sup> for reducing the noise  
359 of low sample size. A linear shrinkage method<sup>34,35</sup> was employed for out-sample reference panel  
360 construction to further reduce the noise. For UKBB real data analysis, the in-sample reference

361 panel was constructed using the union of UKBB imputed genotype panel and UKBB array  
362 genotype panel, intersected with hapmap3 project<sup>39</sup> variant list (N=307,259, M = 966,766) and  
363 the 1009 genomic blocks. For real data analysis, the variant inclusion criteria was (a):  
364 imputation score > 0.8; (b): minor allele frequency > 0.05; (c): missing rate < 0.01; (d): Hardy-  
365 Weinberg Equilibrium P-value > 5\*10<sup>-8</sup>. The details of quality control procedure of simulation  
366 dataset and real analysis dataset can be found in the supplementary materials.

367

### 368 **Simulations**

369 The data generation process followed equation X, with narrow-sense heritability  $h^2_g$  fixed at 0.2,  
370 GE interaction contribution proportion  $h^2_I$  varying from 0 to 0.05, non-genetic-residual-covariate  
371 interaction variance  $\sigma_1^2$  being 0 or 0.02, E is standard normal:

$$Y_i = \sum_{j=1}^M G_{ji} \beta_j + \sum_{j=1}^M S_{ji} \gamma_j + \epsilon_{1i} E_i + \epsilon_{0i},$$

372 For each simulation from the pool of intersected UKBB genotype panel (N=276,050, M =  
373 396,330), we randomly chose 50,000 subjects and 19,816 (5%) causal GE variants for data  
374 generation, association analysis (linear regression on M = 396,330 variants using PLINK2<sup>40</sup>)  
375 and GE interaction variance estimation analysis. Each parameter combination had 300  
376 replicated simulations. To simulate the binary outcome, we used the liability model based on  
377 corresponding critical cutoff with respect to the specified population prevalence.

378

### 379 **Single-covariate GE interaction variance analysis of UKBB**

380 We ran GWIS analysis through “--glm interaction --variance-standardize” command of PLINK2<sup>40</sup>  
381 pre-adjusted for age, sex, 40 genetic PCs and the specific environmental covariate of interest if  
382 not age or sex using linear regression. We analyzed 22 phenotypes and 7 environmental  
383 covariates, resulting in a total of 151 (154 - 3) E-Y pairs with the 3 sex-specific phenotypes. The  
384 22 phenotypes included 14 continuous phenotypes and 8 binary phenotypes. LDER-GE and  
385 LDSC-based analysis were conducted using the resulted GWIS summary statistics and pre-  
386 computed LD information.

387

### 388 **Aggregated multi-covariate GE interaction variance analysis of UKBB**

389 Suppose there is a covariate set of interest (A, B, C, ...), we first run linear regression of B~A to  
390 get residuals of B net A: B|A, being independent from A, and we run another linear regression of  
391 C~A+B to get residuals of C net A and B: C|A & B, being independent from A and B. We

392 continue the process until all residuals are independent from each other. We then run single-  
393 covariate GE interaction variance analysis on each residuals the same way but preadjust for  
394 age, sex, 40 genetic PCs and all covariates in the set excluding age and sex. By eliminating the  
395 dependency of covariates, the estimated single-covariate GE interaction variances are  
396 independent, and we summed up the estimated GE interaction variances and their variances of  
397 estimation to conduct straightforward statistical test. We explored the set (age, sex, BMI,  
398 packed years of smoking, Townsend deprivation index, Alcohol intake frequency) to capture  
399 more missing heritability explained by GE interactions because these 6 covariates yielded  
400 nonminimally significant GE interaction signals at  $P < 0.05$  on more than three phenotype (S  
401 table 6). The narrow-sense heritability of each phenotype was estimated using LDER and the  
402 main genetic effect GWAS summary statistics of the same UKBB cohort as GE analysis.  
403  
404  
405  
406  
407  
408  
409  
410

411 **References**

- 412 1. Hunter, D.J. Gene–environment interactions in human diseases. *Nature reviews genetics* **6**, 287-298 (2005).
- 413 2. Manuck, S.B. & McCaffery, J.M. Gene-environment interaction. *Annual review of*  
414 *psychology* **65**, 41-70 (2014).
- 415 3. Favé, M.-J. et al. Gene-by-environment interactions in urban populations modulate risk  
416 phenotypes. *Nature communications* **9**, 827 (2018).
- 417 4. Dunn, A.R., O'Connell, K.M. & Kaczorowski, C.C. Gene-by-environment interactions in  
418 Alzheimer's disease and Parkinson's disease. *Neuroscience & Biobehavioral Reviews* **103**,  
419 73-80 (2019).
- 420 5. Van IJzendoorn, M.H. et al. Gene-by-environment experiments: a new approach to  
421 finding the missing heritability. *Nature Reviews Genetics* **12**, 881-881 (2011).
- 422 6. Virolainen, S.J., VonHandorf, A., Viel, K.C., Weirauch, M.T. & Kottyan, L.C. Gene–  
423 environment interactions and their impact on human health. *Genes & Immunity* **24**, 1-11  
424 (2023).
- 425 7. Miao, J. et al. Reimagining Gene-Environment Interaction Analysis for Human Complex  
426 Traits. *bioRxiv*, 2022.12. 11.519973 (2022).
- 427 8. Shin, J. & Lee, S.H. GxEsum: a novel approach to estimate the phenotypic variance  
428 explained by genome-wide GxE interaction based on GWAS summary statistics for  
429 biobank-scale data. *Genome biology* **22**, 1-17 (2021).
- 430 9. Gauderman, W.J., Zhang, P., Morrison, J.L. & Lewinger, J.P. Finding novel genes by  
431 testing G × E interactions in a genome – wide association study. *Genetic epidemiology*  
432 **37**, 603-613 (2013).
- 433 10. Wang, H. et al. Genotype-by-environment interactions inferred from genetic effects on  
434 phenotypic variability in the UK Biobank. *Science advances* **5**, eaaw3538 (2019).
- 435 11. Zhang, P., Lewinger, J.P., Conti, D., Morrison, J.L. & Gauderman, W.J. Detecting gene–  
436 environment interactions for a quantitative trait in a genome – wide association study.  
437 *Genetic epidemiology* **40**, 394-403 (2016).
- 438 12. Robinson, M.R. et al. Genotype–covariate interaction effects and the heritability of adult  
439 body mass index. *Nature genetics* **49**, 1174-1181 (2017).
- 440 13. Ni, G. et al. Genotype–covariate correlation and interaction disentangled by a whole-  
441 genome multivariate reaction norm model. *Nature communications* **10**, 2239 (2019).
- 442 14. Bulik-Sullivan, B.K. et al. LD Score regression distinguishes confounding from  
443 polygenicity in genome-wide association studies. *Nature genetics* **47**, 291-295 (2015).
- 444 15. Song, S., Jiang, W., Zhang, Y., Hou, L. & Zhao, H. Leveraging LD eigenvalue regression to  
445 improve the estimation of SNP heritability and confounding inflation. *The American*  
446 *Journal of Human Genetics* **109**, 802-811 (2022).
- 447 16. Ning, Z., Pawitan, Y. & Shen, X. High-definition likelihood inference of genetic  
448 correlations across human complex traits. *Nature genetics* **52**, 859-864 (2020).
- 449 17. Sudlow, C. et al. UK biobank: an open access resource for identifying the causes of a  
450 wide range of complex diseases of middle and old age. *PLoS medicine* **12**, e1001779  
451 (2015).
- 452

453 18. Dempster, E.R. & Lerner, I.M. Heritability of threshold characters. *Genetics* **35**, 212  
454 (1950).

455 19. Simino, J. et al. Gene-age interactions in blood pressure regulation: a large-scale  
456 investigation with the CHARGE, Global BPgen, and ICBP Consortia. *The American Journal  
457 of Human Genetics* **95**, 24-38 (2014).

458 20. Shi, G. et al. Genetic effect on blood pressure is modulated by age: the Hypertension  
459 Genetic Epidemiology Network Study. *Hypertension* **53**, 35-41 (2009).

460 21. Silventoinen, K. et al. Heritability of adult body height: a comparative study of twin  
461 cohorts in eight countries. *Twin Research and Human Genetics* **6**, 399-408 (2003).

462 22. Sjöberg, R.L. et al. Development of depression: sex and the interaction between  
463 environment and a promoter polymorphism of the serotonin transporter gene.  
464 *International Journal of Neuropsychopharmacology* **9**, 443-449 (2006).

465 23. Hornung, O.P. & Heim, C.M. Gene–environment interactions and intermediate  
466 phenotypes: early trauma and depression. *Frontiers in endocrinology* **5**, 14 (2014).

467 24. Cupido, A.J., Asselbergs, F.W., Schmidt, A.F. & Hovingh, G.K. Low - Density Lipoprotein  
468 Cholesterol Attributable Cardiovascular Disease Risk Is Sex Specific. *Journal of the  
469 American Heart Association* **11**, e024248 (2022).

470 25. Taylor, K.C. et al. Investigation of gene-by-sex interactions for lipid traits in diverse  
471 populations from the population architecture using genomics and epidemiology study.  
472 *BMC genetics* **14**, 1-10 (2013).

473 26. Reddon, H., Guéant, J.-L. & Meyre, D. The importance of gene–environment interactions  
474 in human obesity. *Clinical science* **130**, 1571-1597 (2016).

475 27. Nakamura, S. et al. Gene–environment interactions in obesity: implication for future  
476 applications in preventive medicine. *Journal of human genetics* **61**, 317-322 (2016).

477 28. Lim, J.E. et al. Gene–environment interactions related to blood pressure traits in two  
478 community - based Korean cohorts. *Genetic Epidemiology* **43**, 402-413 (2019).

479 29. Hyppönen, E., Mulugeta, A., Zhou, A. & Santhanakrishnan, V.K. A data-driven approach  
480 for studying the role of body mass in multiple diseases: a phenome-wide registry-based  
481 case-control study in the UK Biobank. *The Lancet Digital Health* **1**, e116-e126 (2019).

482 30. Larsson, S.C., Bäck, M., Rees, J.M., Mason, A.M. & Burgess, S. Body mass index and body  
483 composition in relation to 14 cardiovascular conditions in UK Biobank: a Mendelian  
484 randomization study. *European heart journal* **41**, 221-226 (2020).

485 31. Lee, S.H., Wray, N.R., Goddard, M.E. & Visscher, P.M. Estimating missing heritability for  
486 disease from genome-wide association studies. *The American Journal of Human  
487 Genetics* **88**, 294-305 (2011).

488 32. Van Vleck, L. Estimation of heritability of threshold characters. *Journal of Dairy Science*  
489 **55**, 218-225 (1972).

490 33. Siva, N. 1000 Genomes project. *Nature biotechnology* **26**, 256-257 (2008).

491 34. Ledoit, O. & Wolf, M. Spectrum estimation: A unified framework for covariance matrix  
492 estimation and PCA in large dimensions. *Journal of Multivariate Analysis* **139**, 360-384  
493 (2015).

494 35. Ledoit, O. & Wolf, M. Numerical implementation of the QuEST function. *Computational  
495 Statistics & Data Analysis* **115**, 199-223 (2017).

496 36. Berisa, T. & Pickrell, J.K. Approximately independent linkage disequilibrium blocks in  
497 human populations. *Bioinformatics* **32**, 283 (2016).

498 37. Speed, D. & Balding, D.J. SumHer better estimates the SNP heritability of complex traits  
499 from summary statistics. *Nature genetics* **51**, 277-284 (2019).

500 38. Di Scipio, M. et al. A versatile, fast and unbiased method for estimation of gene-by-  
501 environment interaction effects on biobank-scale datasets. *Nature Communications* **14**,  
502 5196 (2023).

503 39. Gibbs, R.A. et al. The international HapMap project. (2003).

504 40. Chang, C.C. et al. Second-generation PLINK: rising to the challenge of larger and richer  
505 datasets. *Gigascience* **4**, s13742-015-0047-8 (2015).

506

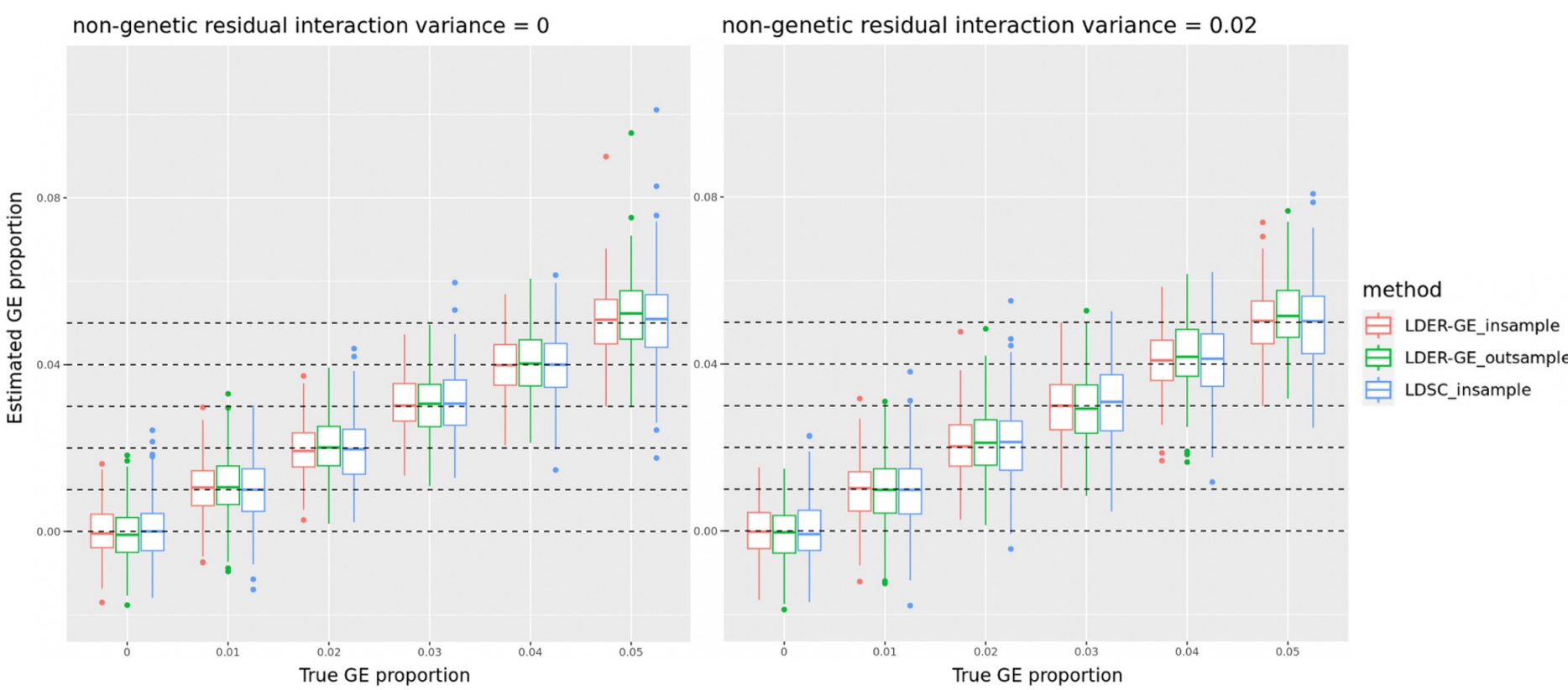


Figure 1: Histogram comparison of LDSC-based method and LDER-GE with in-sample and out-sample reference panel on simulations from real genotype panel, continuous phenotype.

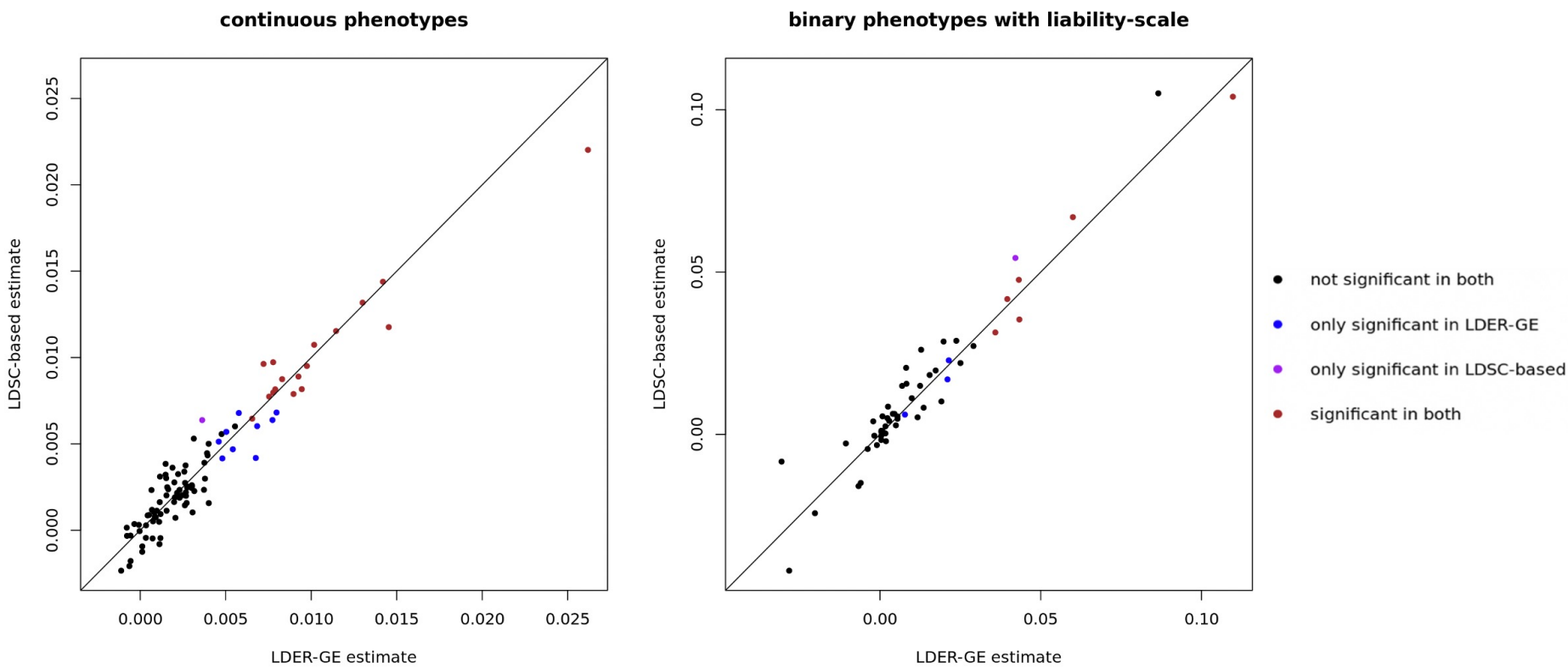


Figure 2: GE interaction variance estimates from LDSC-based method and LDER-GE of 151 environmental covariate-phenotype pairs in UKBB dataset. For binary phenotypes, GE interaction variance is reported on the liability-scale.

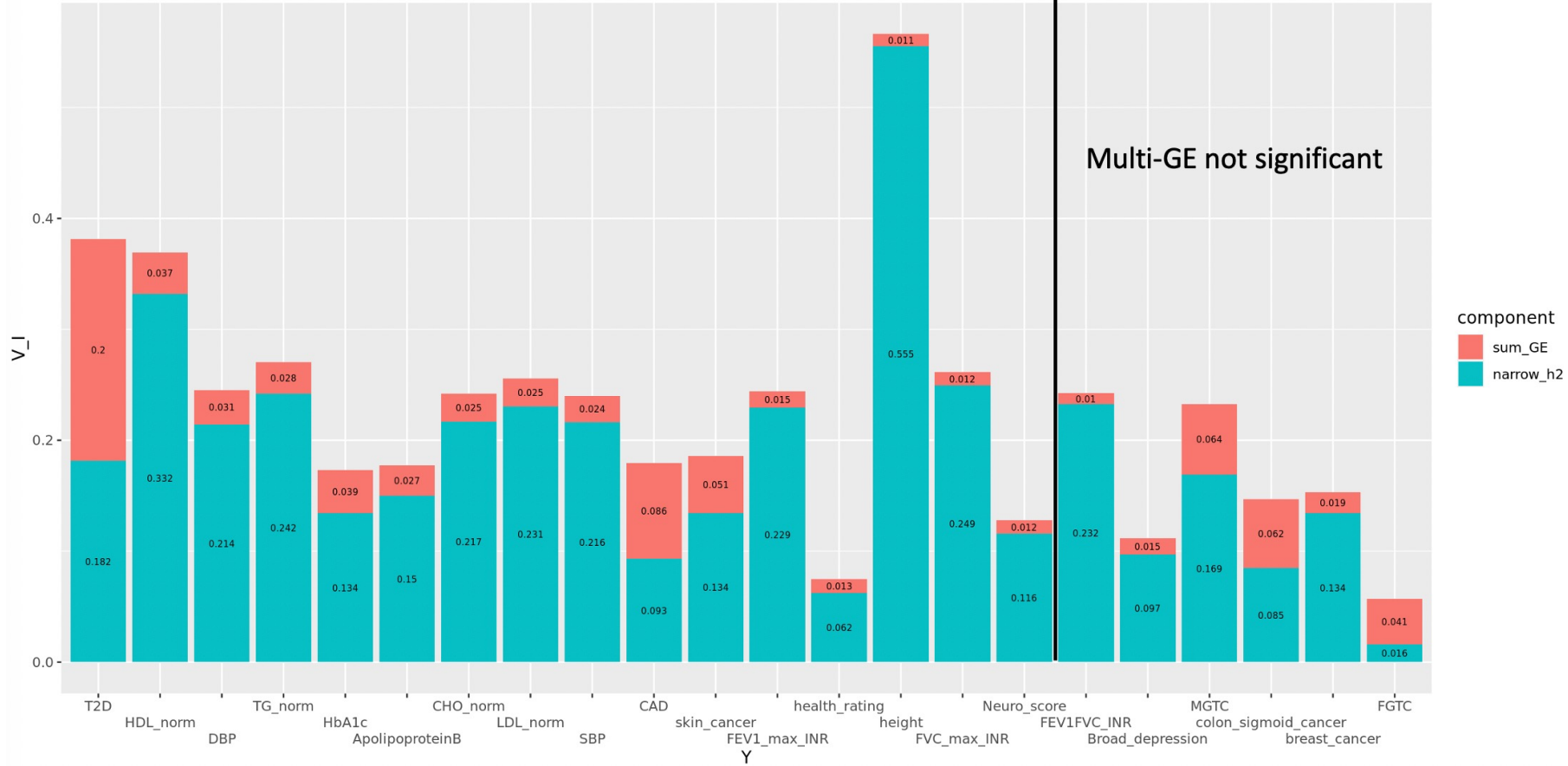


Figure 3: Phenotypic variance explained by narrow-sense heritability and aggregated multi-GE interactions for the 22 phenotypes, ordered by increasing P value of multi-GE interactions. Right of the solid black line, 6 phenotypes are not significant. For binary phenotypes, proportion is reported on the liability-scale.

FGTC: Female genital tract cancer  
 MGTC: Male genital tract cancer